

Lattice model for percolation on a plane of partially aligned sticks with length dispersity

Avik P. Chatterjee*

*Department of Chemistry, SUNY-ESF, One Forestry Drive, Syracuse, NY 13210, USA and
The Michael M. Szwarc Polymer Research Institute, Syracuse, NY 13210, USA*

Yuri Yu. Tarasevich†

Instituto de Física, Universidade Federal Fluminense, Niterói, RJ, Brasil

(Dated: May 24, 2024)

A lattice-based model for continuum percolation is applied to the case of randomly located, partially aligned sticks with unequal lengths in 2D which are allowed to cross each other. Results are obtained for the critical number of sticks per unit area at the percolation threshold in terms of the distributions over length and orientational angle and are compared with findings from computer simulations. Consistent with findings from computer simulations, our model shows that the percolation threshold is (i) elevated by increasing degrees of alignment for a fixed length distribution, and (ii) lowered by increasing degrees of length dispersity for a fixed orientational distribution. The impact of length dispersity is predicted to be governed entirely by the first and second moments of the stick length distribution, and the threshold is shown to be quite sensitive to particulars of the orientational distribution function.

I. INTRODUCTION

The formation of connected networks of microscopic particles (or other entities) that span macroscopic length scales comparable to the dimensions of the system they are embedded in is referred to as percolation and is related to substantial changes in material properties such as electrical conductivity [1–6]. Examination of this subject using theoretical as well as computational methods has a deep history in the field [6–11], and an understanding of conditions conducive to achieving percolation can assist in designing composites with desirable characteristics. Recent computer simulations have modeled effects due to varying the degree of length dispersity of the particles [9, 12] thereby enabling a more realistic picture that accounts for the fact that the ideal situation of identically-sized particles is seldom encountered in experiments. The impact of varying degrees of alignment, which can reflect the conditions under which a material has been processed, has been examined as well in simulations for both two-dimensional (2D) [6, 9, 13, 14] and three-dimensional (3D) systems [15]. The impact of these factors (length dispersity and degree of alignment) upon the percolation threshold is important for predicting the characteristics of thin film conductive structures based upon elongated particles such as carbon nanotubes or metal nanowires [16–24]. In this study we examine the application of a lattice-based theoretical approach [25, 26] for modeling continuum percolation to the situation of partially aligned sticks with unequal lengths that are distributed randomly upon a planar 2D surface.

Our formalism exploits an analogy between lattice and continuum percolation that is based upon preserving the

average number of contacts that lead to connectedness between individual entities. It is a method that has been employed with some success in capturing the impact of length dispersity upon the percolation threshold for rod-like particles in 3D [27], and which has been shown to accurately describe the dependence of the percolation threshold upon aspect ratio for isotropic, equally sized, penetrable rectangles in 2D [26]. In this study we obtain a compact analytical expression for the critical areal density of sticks (rectangles of zero width) at the percolation threshold that accounts in a simple way for distributions over both the lengths of the sticks and their orientational angles. Results from this model are compared with those obtained from computer simulations for the appropriate orientational distributions that were employed in those investigations [6, 9]. Consistent with the simulations, we find that broadening the length distribution (for a fixed average stick length, $\langle L \rangle$) and increasing alignment have antagonistic effects upon the percolation threshold: the former lowers the threshold, while the latter elevates it.

Section II presents our theoretical methodology and the different angular probability distribution functions (PDFs) that we use as illustrative examples and for comparison with simulations. Results from our comparison with computer simulations are presented with our conclusions in Section III. Section IV summarizes our main findings.

II. MODEL FOR PERCOLATION BY PENETRABLE RECTANGLES WITH UNEQUAL LENGTHS

A. Lattice-based model for continuum percolation

We commence by considering a system of rectangles of uniform width (denoted w) and a distribution over

* achatter@esf.edu

† Corresponding author: ytarasevich@id.uff.br

lengths (denoted L) that are located in a spatially random and uncorrelated manner upon a 2D planar surface. The probability distribution function over lengths, denoted $f(L)$, satisfies

$$\int_0^\infty dL f(L) = 1, \quad (1)$$

and moments of the length distribution are denoted

$$\langle L^m \rangle = \int_0^\infty dL f(L) L^m. \quad (2)$$

The rectangles are assumed to be completely interpenetrable and are allowed to overlap, and we denote by ρ the number of rectangles (of all lengths) per unit area. Each overlap between a pair of such (penetrable) rectangles creates a ‘‘contact’’ by virtue of which that pair of objects is defined to be ‘‘connected’’. The excluded area between a pair of rectangles of lengths L_i and L_j is denoted A_{ij} and satisfies

$$A_{ij} = (L_i L_j + w^2) |\sin \gamma| + w(L_i + L_j)(1 + |\cos \gamma|), \quad (3)$$

for a given prescribed value of the angle γ between the longitudinal axes of the pair of objects ([26] cf. [28]). When averaged over the angular PDF for the selected pair of rectangles with lengths L_i and L_j , Eqn. (3) leads to

$$\langle A_{ij} \rangle = (L_i L_j + w^2) \langle |\sin \gamma| \rangle + w(L_i + L_j)(1 + \langle |\cos \gamma| \rangle), \quad (4)$$

where we have assumed that the orientational distribution functions are identical for all values of the lengths so that the averages $\langle |\sin \gamma| \rangle$ and $\langle |\cos \gamma| \rangle$ are independent of the lengths L_i and L_j of the pair of rectangles under consideration. (In the more general case in which the angular PDFs depend upon aspect ratio, the averages of $|\sin \gamma|$ and $|\cos \gamma|$ will depend upon the indices i and j and the terms appearing in (4) must be denoted $\langle |\sin \gamma| \rangle_{ij}$ and $\langle |\cos \gamma| \rangle_{ij}$ instead.) The average number of contacts that a rectangle of length L_i is expected to experience with all of the other rectangles in the system is denoted $n_{c,i}$ and can be estimated from

$$n_{c,i} = \rho \int_0^\infty dL_j f(L_j) \langle A_{ij} \rangle. \quad (5)$$

Our heuristic mapping between the problems of (i) percolation by this system of rectangles and of (ii) percolation on a generalization of the Bethe lattice proceeds as follows [25, 26]. We associate a vertex degree z_i with each possible value of the length L_i and the vertices of the lattice are assumed to be occupied with a uniform probability

$$\xi = \rho w \int_0^\infty dL f(L) = \rho w \langle L \rangle. \quad (6)$$

Each occupied site with vertex degree z_i in the lattice model is intended to represent a rectangle of length L_i . The vertex degrees are related to the lengths by imposing the requirement that the average number of contacts be the same within the different models, that is

$$z_i = \frac{n_{c,i}}{\xi} = \frac{1}{w \langle L \rangle} \int_0^\infty dL_j f(L_j) \langle A_{ij} \rangle. \quad (7)$$

Equations (4) and (7) lead to

$$z_i = \left(\frac{L_i}{w} + \frac{w}{\langle L \rangle} \right) \langle |\sin \gamma| \rangle + \left(\frac{L_i}{\langle L \rangle} + 1 \right) (1 + \langle |\cos \gamma| \rangle). \quad (8)$$

Within the assumption that closed loops can be neglected and that the lattice can be treated as being tree-like, our problem transforms to that of percolation on a Bethe lattice with a distribution over vertex degrees that reflects the distribution over lengths for the system of rectangles, and with a site occupation probability given by ξ . The critical site occupation probability at the percolation threshold for such a lattice, denoted ξ_c , is given [25, 29, 30] by

$$\xi_c = \frac{\langle z \rangle}{\langle z^2 \rangle - \langle z \rangle}, \quad (9)$$

where $\langle z \rangle$ and $\langle z^2 \rangle$ are the average values of the vertex degree and square of the vertex degree, respectively, averaged over all the vertices in the lattice. From (8) we find that

$$\langle z \rangle = \frac{1}{w \langle L \rangle} \times [(\langle L \rangle^2 + w^2) \langle |\sin \gamma| \rangle + 2w \langle L \rangle (1 + \langle |\cos \gamma| \rangle)], \quad (10)$$

and

$$\langle z^2 \rangle = (\varepsilon^2 P + 2 + \varepsilon^{-2}) \langle |\sin \gamma| \rangle^2 + (P + 3) (1 + \langle |\cos \gamma| \rangle)^2 + 2 (\varepsilon P + \varepsilon + 2\varepsilon^{-1}) \langle |\sin \gamma| \rangle (1 + \langle |\cos \gamma| \rangle), \quad (11)$$

where

$$P = \frac{\langle L^2 \rangle}{\langle L \rangle^2},$$

while

$$\varepsilon = \frac{\langle L \rangle}{w}$$

is the aspect ratio. Equations (9), (10), and (11) yield

$$\rho_c \langle L \rangle^2 = \frac{\varepsilon \langle z \rangle}{\langle z^2 \rangle - \langle z \rangle} = \varepsilon \xi_c, \quad (12)$$

where $\langle z \rangle$ and $\langle z^2 \rangle$ are given by (10) and (11). It is straightforward but tedious to verify from (10) and (11) that $\langle z^2 \rangle > 2\langle z \rangle$ for any choice of the angular PDF and hence that the critical value of the site occupation probability ξ_c is always smaller than unity, as it ought to be.

The result in (10), (11), and (12) simplifies considerably in the limit of vanishing widths (or very large aspect ratios), which we refer to as the “stick limit”. If one takes the limit $w \rightarrow 0$ for fixed choices of the angular PDF and length distribution function $f(L)$, (10), (11), and (12) lead to

$$\rho_c^{\text{stick}} \langle L \rangle^2 = \frac{P}{\langle |\sin \gamma| \rangle} = \frac{1}{(1 + \Sigma^2) \langle |\sin \gamma| \rangle}, \quad (13)$$

where $\Sigma = \sigma_L / \langle L \rangle$, while σ_L denotes the standard deviation in the lengths of the sticks. The factorization of the result in (12) into parts that depend exclusively upon (i) the length dispersity and (ii) the angular PDFs arises from our assumption that the angular PDFs are independent of the stick lengths. For an isotropic orientational distribution in two dimensions $\langle |\sin \gamma| \rangle = \langle |\cos \gamma| \rangle = 2/\pi$, and (13) reduces to

$$\rho_{c,\text{iso}}^{\text{stick}} \langle L \rangle^2 = \frac{\pi}{2} P. \quad (14)$$

For the case of perfectly aligned rectangles for which $\gamma \equiv 0$, (9), (10), (11), and (12) yield

$$\rho_{c,\text{aligned}} \langle L \rangle^2 = \frac{\varepsilon}{P + 2}, \quad (15)$$

which remains finite so long as the width w is greater than zero.

B. Examples of Angular Distribution Function

Ascertaining the exact angular distribution function for elongated particles for a real experimental system is, in general, an arduous and difficult task [20, 24, 31, 32]. Under most circumstances complete information regarding the angular distribution is not readily available. In view of this reality we have chosen a number of different angular PDFs to model possible orientational distributions. Within the assumption that the angular PDF is independent of the stick length we find that the dependence (as opposed to the absolute value) of the threshold upon length dispersity is independent of the particular PDF that is chosen and is governed by the scaled standard deviation of the stick length, namely Σ . Additionally, our model predicts that the threshold depends upon length dispersity exclusively through Σ regardless of the distribution function describing the stick lengths.

As simple models for the state of alignment of the rectangles, we employ the four following illustrative angular PDFs $g(\theta)$, which we designate as angular PDFs A, B, C, and D.

a. Angular PDF A. This representation envisages the following step function structure for $g(\theta)$

$$g(\theta) = \begin{cases} \frac{1}{2\alpha}, & \text{for } |\theta| \leq \alpha, \\ 0, & \text{for } |\theta| > \alpha, \end{cases} \quad (16)$$

where $\alpha \leq \pi/2$ and the angular PDF is normalized such that

$$\int_{-\pi/2}^{\pi/2} d\theta g(\theta) = 1.$$

For this choice of angular PDF the orientational order parameter, denoted S , satisfies

$$S = \langle \cos 2\theta \rangle = \frac{\sin 2\alpha}{2\alpha}, \quad (17)$$

and the averages $\langle |\sin \gamma| \rangle$ and $\langle |\cos \gamma| \rangle$ are given by [26]

$$\langle |\sin \gamma| \rangle = \frac{1}{\alpha} \left(1 - \frac{\sin 2\alpha}{2\alpha} \right), \quad (18)$$

and

$$\langle |\cos \gamma| \rangle = \begin{cases} \frac{1 - \cos 2\alpha}{2\alpha^2}, & \text{for } \alpha \leq \frac{\pi}{4}, \\ \frac{4\alpha - \pi + 1 + \cos 2\alpha}{2\alpha^2}, & \text{for } \alpha \geq \frac{\pi}{4}. \end{cases} \quad (19)$$

b. Angular PDF B. This approximation was employed in prior investigations [9, 14] and envisages a normal (Gaussian) distribution over orientation angles as follows

$$g(\theta) = \frac{1}{\sqrt{-\pi \ln S}} \exp \left(\frac{\theta^2}{\ln S} \right), \quad (20)$$

for which the variance in the angles θ is given by $\text{Var}(\theta) = -0.5 \ln S$. For this choice of angular PDF, averages such as $\langle |\sin \gamma| \rangle$ and $\langle |\cos \gamma| \rangle$ must be calculated by numerical integration.

c. Angular PDF C. In this approximation the angular PDF is approximated by a pair of symmetrically distributed Dirac delta functions as follows

$$g(\theta) = \frac{1}{2} [\delta(\theta - \alpha) + \delta(\theta + \alpha)], \quad (21)$$

where α is selected to reproduce desired values for the orientational order parameter S . For any prescribed value of S , angular PDF C has the smallest possible variance in the angle made by the longitudinal axes of the rectangles with the alignment direction, and we find that

$$\langle |\sin \gamma| \rangle = \frac{1}{2} \sqrt{1 - S^2} \quad (22)$$

and

$$\langle |\cos \gamma| \rangle = \frac{1}{2} (1 + S). \quad (23)$$

d. Angular PDF D. In this approximation the angular PDF is represented by a pair of Dirac delta functions that are aligned parallel and perpendicular to the alignment direction

$$g(\theta) = f_0\delta(\theta) + (1 - f_0)\delta\left(\theta - \frac{\pi}{2}\right), \quad (24)$$

where the weight factor f_0 is selected to reproduce desired values of the orientational order parameter S . For any prescribed value of S , angular PDF D has the largest possible variance in the angle made by the longitudinal axes of the rectangles with the alignment direction, and we find that

$$\langle |\sin \gamma| \rangle = \frac{1}{2}(1 - S^2) \quad (25)$$

and

$$\langle |\cos \gamma| \rangle = \frac{1}{2}(1 + S^2). \quad (26)$$

It should be noted that the choice $S = 0$ reduces to an isotropic distribution for PDFs A and B, but not for C and D. Our choices for angular PDFs are intended to be illustrative and are not by any means exhaustive, and other choices are possible and have been investigated [13, 21, 32].

III. RESULTS

In comparing our findings with published results of computer simulations, we focus attention on the case of rectangles with zero-width, namely, the stick limit (13). For the case of sticks that are equally sized and isotropically oriented, simulations have shown [33] that $\rho_c L^2 = 5.63724$ whereas our model yields $\rho_c L^2 = \pi/2$ for PDF A (16), while $\rho_c L^2 = 1/2$ for PDF C (22) and PDF D (25). In order to compare various results in a way that examines the dependence (as opposed to the absolute value) of ρ_c upon system variables, we multiply our result in (13) by an appropriate factor, ρ_0 ,

$$\rho_c^{\text{stick}} \langle L \rangle^2 = \frac{\rho_0}{(1 + \Sigma^2) \langle |\sin \gamma| \rangle}. \quad (27)$$

Our choice for the factor ρ_0 depends on particular choice of angular PDF. The choice of the prefactor in (27) enforces quantitative agreement between our model and the simulation-derived results for equally sized sticks for which $S = 0$ [33], and enables focusing upon relative variations in ρ_c instead. For an isotropic system of equal-length sticks, $\sigma_L^2 = 0$, $\langle L \rangle = L$, hence,

$$\rho_c^{\text{stick}} L^2 = \frac{\rho_0}{\langle |\sin \gamma| \rangle}.$$

Equation (18) yields

$$\lim_{\alpha \rightarrow 0} \langle |\sin \gamma| \rangle = \lim_{\alpha \rightarrow 0} \frac{1}{\alpha} \left(1 - \frac{\sin 2\alpha}{2\alpha}\right) = \frac{2}{3}\alpha,$$

hence,

$$\rho_c^{\text{stick}} L^2 = \frac{3\rho_0}{2\alpha}. \quad (28)$$

The effect of partial alignment upon the percolation threshold for equally sized sticks for the stepfunction angular PDF (PDF A) is shown in Fig. 1. The computer simulation study reported in Yook *et al.* [6] found that for this choice of angular PDF (i) $\rho_c L^2$ depended only weakly upon the cutoff angle α for $\alpha \geq 5\pi/18$, but that (ii) for $\alpha < 5\pi/18$ the threshold increased with the degree of alignment, approximately following $\rho_c L^2 \propto \alpha^{-0.9}$. Our results are qualitatively similar to these findings with the distinction that (18) and (27) predict that for high degrees of alignment ($\alpha \gtrsim 0.4$), $\rho_c L^2 \propto \alpha^{-1}$ instead. The dashed line in Fig. 1 denotes the behavior $\rho_c L^2 = 5.38\alpha^{-1}$. For highly anisotropic systems ($\alpha \gtrsim 1.1$), variation in the percolation threshold is less than 10% (dotted line depicts the value $1.1\rho_c^{\text{iso}} L^2$). Our findings are qualitatively consistent with the observations reported in [6].

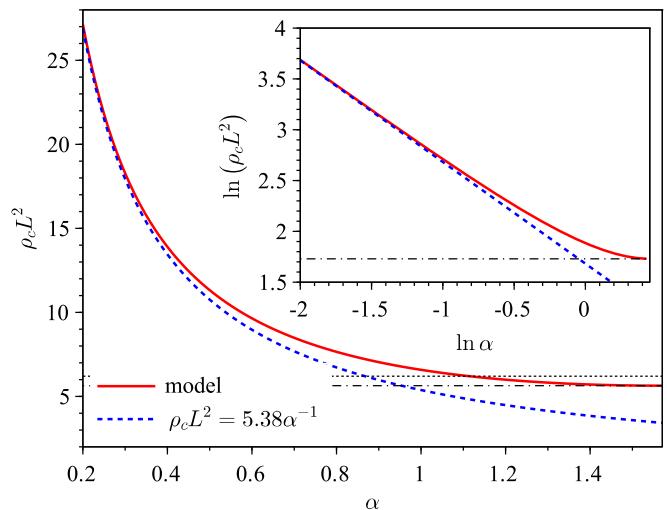


FIG. 1. The solid line depicts the percolation threshold for equally sized, partially aligned sticks calculated from (18) and (27) for angular PDF A (16) as a function of the cutoff angle α . The dashed line depicts the behaviors $\rho_c L^2 = 5.38\alpha^{-1}$ (28). Dash-dot line corresponds to the percolation threshold for isotropic systems. The horizontal dotted line corresponds to the threshold for isotropic systems multiplied by the factor 1.1.

The combined effects of both length dispersity and alignment upon the percolation threshold have been examined in the simulation study reported in [9], which investigated a log-normal distribution over stick lengths and a Gaussian distribution (angular PDF B in the present account) over stick angular orientations. Figure 2 depicts the dependence of the normalized percolation threshold

$$\frac{\rho_c \langle L \rangle^2}{(\rho_c \langle L \rangle^2)_{\Sigma=0}} = \frac{1}{1 + \Sigma^2} \quad (29)$$

upon dispersity in the stick lengths for various prescribed, fixed value of the order parameter S . (The value of $\langle |\sin \gamma| \rangle$ for a given value of S is different depending upon the PDF that is used.) The line represents calculations from our model (29). Markers represent simulation results from [9]) for $S = 0.9, 0.5, 0$. Increasing the dispersity in stick lengths (quantified by Σ) for any value of S always lowers the threshold. The results from the simulation [9] collapse onto a single curve for each value of S , thereby exhibiting the dependence upon Σ predicted by our model.

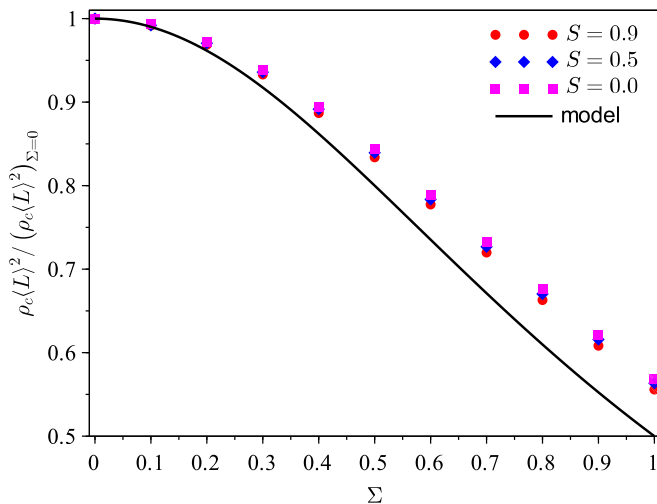


FIG. 2. The percolation threshold $\rho_c \langle L \rangle^2 / (\rho_c \langle L \rangle^2)_{\Sigma=0}$ is shown as a function of the degree of length dispersity of the sticks (Σ) for fixed values of the orientational order parameter S . The markers represent the simulation results from Ref. 9 for values of $S = 0.9, 0.5, 0$. The line represents calculations from our model (29).

Figure 3 reveals that results from the simulations of Ref. 9 are in close agreement with those obtained from our model using the same angular PDF (PDF B). The sensitivity of the predicted values of $\rho_c \langle L \rangle^2$ to the choice of angular PDF for high degrees of stick alignment is demonstrated in Supplemental Material [URL will be inserted by publisher]. For the calculations depicted in Fig. 3 that employ the Gaussian angular PDF (PDF B), the quantity $\langle |\sin \gamma| \rangle$ required in evaluating the right-hand-side of (27) is obtained by numerical integration.

The dependence of

$$\frac{\rho_c \langle L \rangle^2}{(\rho_c \langle L \rangle^2)_{S=0}} = \frac{1}{\langle |\sin \gamma| \rangle} \quad (30)$$

upon the extent of alignment (quantified by S) for various fixed degrees of length dispersity (Σ) is shown in Fig. 4. Consistent with the findings depicted in Fig. 1, the threshold is seen to increase steeply with increasing degrees of alignment especially for large values of S . Results from our Gaussian PDF (PDF B) (the solid line in Fig. 4) are again similar to those reported in Ref. 9.

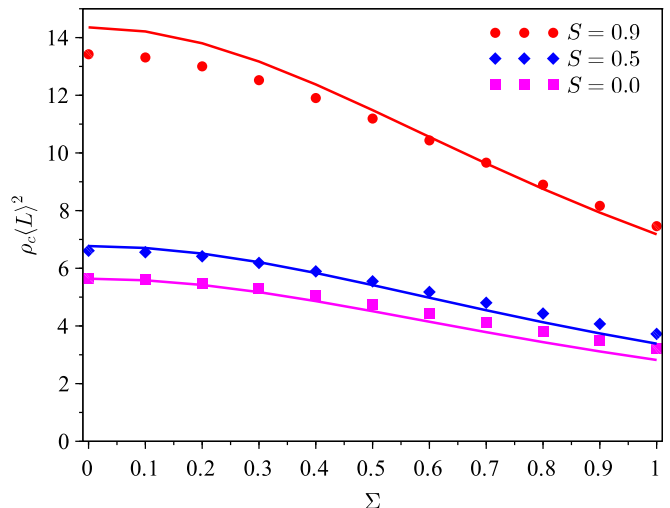


FIG. 3. The percolation threshold $\rho_c \langle L \rangle^2$ is shown as a function of the degree of lengths dispersity of the sticks (Σ) for different values of the orientational order parameter $S = 0.9, 0.5, 0$. The markers represent the simulation results from Ref. 9. The lines represent calculations from our model (27) using angular PDF B.

Results from the simulations [9] and from model calculations for each PDF for different length dispersities collapse onto individual curves that depend only upon the value of S . (It should be noted that in our model $\rho_c \langle L \rangle^2$ vanishes in the limits that either (i) $\langle L^2 \rangle / \langle L \rangle^2 \rightarrow \infty$, or (ii) $S \rightarrow 0$.) Increasing dispersity at a fixed value of $\langle L \rangle$ implies the presence of larger fractions of longer sticks that have a higher likelihood to cross and form contacts, thereby lowering the areal number density at the threshold. A comparable phenomenon has been reported for the case of (isotropic and random) rod-like particles in 3D, for which the weight-averaged aspect ratio was found to govern the percolation threshold [27].

IV. CONCLUSIONS

In concluding, we have extended a lattice-based model for continuum percolation to describe penetrable rectangles and zero-width sticks in 2D. Despite the fact that our approach neglects the impact of closed loops of connected objects, our results successfully describe major features of the dependence of the percolation threshold upon dispersity in the stick lengths and degree of alignment observed in computer simulation studies. In particular, the dependence upon the length distribution is predicted to be governed by the first and second moments of the stick length through the ratio $\sigma_L / \langle L \rangle$ for any length distribution function, which is consistent with and generalizes existing findings for the log-normal distribution [9, 12]. Our approach assigns a central role to the excluded area, and can be extended to other situations where estimates for this quantity are available. For situations where only

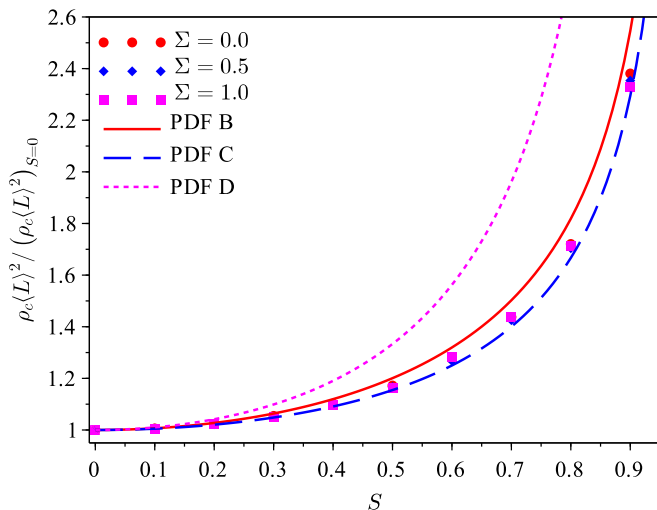


FIG. 4. The percolation threshold $\rho_c(L)^2$ is shown as a function of the degree of alignment (S) of the sticks for fixed values of the dispersity in stick lengths (Σ). The diamonds, squares, and triangles represent the simulation results from [9] for $\Sigma = 1.0, 0.5, 0$, respectively. The solid, dashed, and dotted lines represent calculations from our model (27) using angular PDFs B, C, and D, respectively.

incomplete information is available about the length dispersity and angular PDFs, our study nevertheless identifies: (i) trends in the dependence of the threshold upon S and Σ , and (ii) bounds (ascertained from the angular PDFs C and D) within which the threshold can vary for a prescribed value of S . The trends identified in our model are consistent with those reported from simulations [6, 9, 12].

ACKNOWLEDGMENTS

We acknowledge funding from the FAPERJ, Grants No. E-26/202.666/2023 and No. E-26/210.303/2023 (Y.Y.T.).

-
- [1] I. Balberg and N. Binenbaum, Computer study of the percolation threshold in a two-dimensional anisotropic system of conducting sticks, *Phys. Rev. B* **28**, 3799 (1983).
 - [2] J. W. Borchert, I. E. Stewart, S. Ye, A. R. Rathmell, B. J. Wiley, and K. I. Winey, Effects of length dispersity and film fabrication on the sheet resistance of copper nanowire transparent conductors, *Nanoscale* **7**, 14496 (2015).
 - [3] F. Carmona and A. El Amarti, Anisotropic electrical conductivity in heterogeneous solids with cylindrical conducting inclusions, *Phys. Rev. B* **35**, 3284 (1987).
 - [4] F. Du, J. E. Fischer, and K. I. Winey, Effect of nanotube alignment on percolation conductivity in carbon nanotube/polymer composites, *Phys. Rev. B* **72**, 121404(R) (2005).
 - [5] M. Majidian, C. Grimaldi, L. Forró, and A. Magrez, Role of the particle size polydispersity in the electrical conductivity of carbon nanotube-epoxy composites, *Sci. Rep.* **7**, 12553 (2017).
 - [6] S.-H. Yook, W. Choi, and Y. Kim, Conductivity of stick percolation clusters with anisotropic alignments, *J. Korean Phys. Soc.* **61**, 1257 (2012).
 - [7] I. Balberg, N. Binenbaum, and S. Bozowski, Anisotropic percolation in carbon black-polyvinylchloride composites, *Solid State Commun.* **47**, 989 (1983).
 - [8] A. P. Chatterjee, Percolation in polydisperse systems of aligned rods: A lattice-based analysis, *J. Chem. Phys.* **140**, 204911 (2014).
 - [9] Y. Y. Tarasevich and A. V. Eserkepov, Percolation of sticks: Effect of stick alignment and length dispersity, *Phys. Rev. E* **98**, 062142 (2018).
 - [10] D. Stauffer and A. Aharony, *Introduction to Percolation Theory* (Taylor & Francis, London, 1992).
 - [11] I. Balberg, Principles of the theory of continuum percolation, in *Encyclopedia of Complexity and Systems Science* (Springer Berlin Heidelberg, 2020) pp. 1–61.
 - [12] M. A. Bissett, Y. Deng, I. A. Kinloch, and W. W. Sampson, Percolation threshold of clustered, oriented and polydisperse sticks in a plane, *Adv. Theory Simul.* **6**, 2300131 (2023).
 - [13] M. A. Klatt, G. E. Schröder-Turk, and K. Mecke, Anisotropy in finite continuum percolation: threshold estimation by Minkowski functionals, *J. Stat. Mech. Theory Exp.* **2017**, 023302 (2017).
 - [14] O. Gotesdyner, B. Gross, D. Vaknin Ben Porath, and S. Havlin, Percolation on spatial anisotropic networks, *J. Phys. A: Math. Theor.* **55**, 254003 (2022).
 - [15] S. S. Rahatekar, M. S. Shaffer, and J. A. Elliott, Modelling percolation in fibre and sphere mixtures: Routes to more efficient network formation, *Compos. Sci. Technol.* **70**, 356 (2010).
 - [16] M. Engel, J. P. Small, M. Steiner, M. Freitag, A. A. Green, M. C. Hersam, and P. Avouris, Thin film nanotube transistors based on self-assembled, aligned, semiconducting carbon nanotube arrays, *ACS Nano* **2**, 2445 (2008).
 - [17] J. Hicks, A. Behnam, and A. Ural, Resistivity in percolation networks of one-dimensional elements with a length distribution, *Phys. Rev. E* **79**, 012102 (2009).
 - [18] M. Jagota and N. Tansu, Conductivity of nanowire arrays under random and ordered orientation configurations, *Sci. Rep.* **5**, 10219 (2015).
 - [19] T. Sannicolo, M. Lagrange, A. Cabos, C. Celle, J. Simonato, and D. Bellet, Metallic nanowire-based trans-

- parent electrodes for next generation flexible devices: a review, *Small* **12**, 6052 (2016).
- [20] T. Ackermann, R. Neuhaus, and S. Roth, The effect of rod orientation on electrical anisotropy in silver nanowire networks for ultra-transparent electrodes, *Sci. Rep.* **6**, 34289 (2016).
- [21] M. Jagota and I. Scheinfeld, Analytical modeling of orientation effects in random nanowire networks, *Phys. Rev. E* **101**, 012304 (2020).
- [22] J. Dong and I. A. Goldthorpe, Exploiting both optical and electrical anisotropy in nanowire electrodes for higher transparency, *Nanotechnology* **29**, 045705 (2017).
- [23] A. Redondo, N. Mortensen, K. Djeghdi, D. Jang, R. D. Ortuso, C. Weder, L. T. J. Korley, U. Steiner, and I. Gunkel, Comparing percolation and alignment of cellulose nanocrystals for the reinforcement of polyurethane nanocomposites, *ACS Appl. Mater. Interfaces* **14**, 7270 (2022).
- [24] Y. Hu, F. Hu, Y. Chen, H. Gao, W. Liu, K. Zhou, Z. Min, and W. Zhu, Shear force strategy for preparation of aligned silver nanowire transparent conductive thin films, *Colloid Interface Sci. Commun.* **52**, 100685 (2023).
- [25] A. P. Chatterjee, Geometric percolation in polydisperse systems of finite-diameter rods: Effects due to particle clustering and inter-particle correlations, *J. Chem. Phys.* **137**, 134903 (2012).
- [26] A. P. Chatterjee, Percolation thresholds and excluded area for penetrable rectangles in two dimensions, *J. Stat. Phys.* **158**, 248 (2014).
- [27] B. Nigro, C. Grimaldi, P. Ryser, A. P. Chatterjee, and P. van der Schoot, Quasiuniversal connectedness percolation of polydisperse rod systems, *Phys. Rev. Lett.* **110**, 015701 (2013).
- [28] I. Balberg, C. H. Anderson, S. Alexander, and N. Wagner, Excluded volume and its relation to the onset of percolation, *Phys. Rev. B* **30**, 3933 (1984).
- [29] R. Cohen, K. Erez, D. ben-Avraham, and S. Havlin, Resilience of the internet to random breakdowns, *Phys. Rev. Lett.* **85**, 4626 (2000).
- [30] M. E. J. Newman, S. H. Strogatz, and D. J. Watts, Random graphs with arbitrary degree distributions and their applications, *Phys. Rev. E* **64**, 026118 (2001).
- [31] O. Trotsenko, A. Tokarev, A. Gruzd, T. Enright, and S. Minko, Magnetic field assisted assembly of highly ordered percolated nanostructures and their application for transparent conductive thin films, *Nanoscale* **7**, 7155 (2015).
- [32] T. Tomiyama, Y. Seri, and H. Yamazaki, Relationship between wire orientation and optical and electrical anisotropy in silver nanowire/polymer composite films, *Appl. Surf. Sci.* **469**, 340 (2019).
- [33] J. Li and M. Östling, Percolation thresholds of two-dimensional continuum systems of rectangles, *Phys. Rev. E* **88**, 012101 (2013).